# Perceptual Colour Correlogram and Perception-based Statistical Features of Colour Textures

Submitted: 4th November 2014; accepted 10th December 2014;

Konrad Bojar

DOI: 10.14313/JAMRIS_1-2015/2

**Abstract:**
*In this paper a novel definition and understanding of colour correlogram has been proposed. The proposed colour correlogram generalizes the spatial graylevel dependency matrix (SGLDM) to the case of colour textures. This generalization is based on perceptual colour difference measure expressed in the language of the CIELab colour space components. Application of the colour difference instead of arbitrary colour indices or colour components themselves allows to avoid colour-shuffling palletization and introduction of multidimensional objects, respectively; the proposed perceptual colour correlogram is a single 2D matrix. At the same time, a simple relation of the proposed colour correlogram to the spatial graylevel dependency matrix for graylevel textures is retained. Based on this relation it will be shown that there exists a vector of statistical features built from the perceptual colour correlogram which can be used to describe textures in perceptual terms. These statistical features and their abovementioned perceptual interpretation generalize Haralick concepts derived for the SGLDM.*

**Keywords:** *perceptual colour correlogram, perceptual texture features, colour texture classification*

## 1. Introduction

Colour images acquired in the visible range of electromagnetic spectrum are the cheapest and at the same time the most reliable source of measurements for numerous branches of robotics, including environment perception, mapping, simultaneous localization and mapping, intelligent object manipulation, etc. The ratio of quality and accuracy of measurement data to price of the detector is for digital cameras significantly higher compared to the same ratio for ultrasonic sensors and laser scanners of equivalent spatial range and scanning resolution. In fact, actual price of solutions incorporating visual cameras in the system is substantial effort needed to design and engineer suitable measurement image analysis methods and algorithms. This refers especially to the task of detection, segmentation, and classification of objects of interest. In order to enhance efficacy and efficiency of algorithms it is often decided to employ more than one sensor. In most cases, the second sensor is another visible range camera forming a stereo pair with the first one, or a laser scanner allowing generation of RGB-D images. However, supplementing visible range cameras with auxiliary sensors does not eliminate difficulties to discern textures on flat surfaces, mostly in the far field area of the scene.

The above reasoning leads to the conclusion that texture analysis in an arbitrary region of interest (ROI) is still a problem with no satisfactory and universal solution. In practice the ROI may happen to be very irregular – topologically not connected, and of non-smooth boundary. Irregularity of the ROI is a substantial problem for methods based on global transformations [4], such as Fourier or wavelet transformation, or on resolution pyramids. For irregular ROIs far better results are obtained by local (pixel-based [4]) methods. Such methods do not require the ROI to be very regular, as far as it does not contain significantly many holes of size comparable to the size of pixel neighborhood system used in calculations. Such methods are often based on statistical texture features where during calculation process of statistics the ROIs boundary, and in particular – shape of this boundary, do not yield any significant contribution to the final feature value. Most commonly used texture features satisfying this condition are based on histogram [11] or on more general concept of SGLDM [5], or on colour correlogram [6], colour cooccurrence matrix [1], and local binary patterns [9]. This class of features is implementation-friendly due to its parallelization potential and no necessity of exhaustive floating-point computations.

In this paper we propose a novel form of colour correlogram and new statistical features of construction similar to SGLDM-based features. The proposed colour correlogram and its derived features retain perceptual interpretation of the SGLDM and its derived features [5], respectively. This property distinguishes our concept of correlogram from other correlograms known in literature.

Organization of the subsequent is as follows. Section 2 contains a brief overview of existing correlograms, in both grayscale and colour. In Section 2.1 the SGLDM and Haralick features as a basis or our definitions are described. In Section 2.2 I outline colour correlogram definitions and point out their flaws. In Section 3 I propose perceptual colour correlogram and introduce its several statistical features with elaboration of their perceptual interpretation. In Section 4 I discuss results of simple numerical experiments revealing typical perceptual colour correlogram form and typical texture feature values. Section 5 contains summary and conclusions.

## 2. The SGLDM and Colour Correlograms: Existing Methods

Spatial GrayLevel Dependency Matrix (SGLDM) defined in Haralick's paper [5] is a common base for all basic concepts and objects discussed in this paper. Texture features calculated from this matrix are still successfully applied for texture analysis and classification [3, 12]. Currently known generalizations of the SGLDM to the colour domain comprise colour correlogram [6] and colour cooccurrence matrix [1]. Colour correlogram relies on palletization (indexing) process of colours and calculation of the SGLDM of the resultant texture, and colour cooccurrence matrix is in fact a set of SGLDMs, one per every colour channel pair.

All abovementioned concepts are introduced in this section.

### 2.1. The SGLDM and Haralick Features for Grayscale Textures

Let $\boldsymbol{X}$ be a subset of two dimensional integer lattice $\mathbb{Z}^2$, let $\boldsymbol{I} = \{\boldsymbol{0}, \dots \boldsymbol{N}-\boldsymbol{1}\}$ be the set of $\boldsymbol{N}$ graylevels, and let $\boldsymbol{H}: \boldsymbol{X} \to \boldsymbol{I}$ be a texture. We assume that the integer lattice $\mathbb{Z}^2$ is endowed with the maximum metric $\boldsymbol{\rho}$. In order to be more specific, the metric $\boldsymbol{\rho}$ is a function which for arbitrary $\boldsymbol{x}, \boldsymbol{y} \in \mathbb{Z}^2$, $\boldsymbol{x} = (\boldsymbol{x_1}, \boldsymbol{x_2})$, and $\boldsymbol{y} = (\boldsymbol{y_1}, \boldsymbol{y_2})$ is defined by

$$\boldsymbol{\rho}(\boldsymbol{x}, \boldsymbol{y}) = \mathbf{max}(|\boldsymbol{x_1} - \boldsymbol{x_2}|, |\boldsymbol{y_1} - \boldsymbol{y_2}|). \tag{1}$$

Let $\mathbf{Card}\,\boldsymbol{S}$ denote cardinality of an arbitrary set $\boldsymbol{S}$. The above notation allows us to introduce the SGLDM $\boldsymbol{M^d}$ by means of the following formula

$$\boldsymbol{M^d}(\boldsymbol{i}, \boldsymbol{j}) = \boldsymbol{Card}\{(\boldsymbol{x}, \boldsymbol{y}) \mid \boldsymbol{x}, \boldsymbol{y} \in \boldsymbol{X}, \boldsymbol{\rho}(\boldsymbol{x}, \boldsymbol{y}) = \boldsymbol{d}, \boldsymbol{H}(\boldsymbol{x}) = \boldsymbol{i}, \boldsymbol{H}(\boldsymbol{y}) = \boldsymbol{j}\}, \tag{2}$$

where $\boldsymbol{d}$ is a free parameter. We will not consider directional dependency of texture, hence orientation parameter $\boldsymbol{\theta}$ present in a more general version of the SGLDM is omitted. It is straightforward that $\boldsymbol{M^0}$ is diagonal and this diagonal is simply the histogram of the texture $\boldsymbol{H}$. Therefore SGLDM should be considered as a generalization of histogram. Moreover, from the definition (2) it follows that the matrix $\boldsymbol{M^d}$ is symmetric. It the subsequent text we will omit the superscript $\boldsymbol{d}$ as far as it is clear which particular value of $\boldsymbol{d}$ is being concerned or when value of $\boldsymbol{d}$ is arbitrary.

Each and every matrix $\boldsymbol{M^d}$ induces a two-dimensional probability density function (PDF) $\boldsymbol{p}$ by the following normalization:

$$\boldsymbol{p}(\boldsymbol{i}, \boldsymbol{j}) = \frac{\boldsymbol{M}(\boldsymbol{i}, \boldsymbol{j})}{\sum_{(\boldsymbol{k}, \boldsymbol{l}) \in \boldsymbol{I}^2} \boldsymbol{M}(\boldsymbol{k}, \boldsymbol{l})}. \tag{3}$$

In order to simplify further considerations, let us introduce the following marginal distributions of the PDF $\boldsymbol{p}$:

$$\boldsymbol{p}_{\boldsymbol{x}-\boldsymbol{y}}(\boldsymbol{i}) = \sum_{|\boldsymbol{k}-\boldsymbol{l}|=\boldsymbol{i}} \boldsymbol{p}(\boldsymbol{k}, \boldsymbol{l}),, \tag{4}$$

$$\boldsymbol{p_x}(\boldsymbol{i}) = \sum_{\boldsymbol{l}} \boldsymbol{p}(\boldsymbol{i}, \boldsymbol{l}), \tag{5}$$

$$\boldsymbol{p_y}(\boldsymbol{i}) = \sum_{\boldsymbol{k}} \boldsymbol{p}(\boldsymbol{k}, \boldsymbol{i}). \tag{6}$$

By means of the above PDFs, for every texture $\boldsymbol{H}$ and distance value $\boldsymbol{d}$ the following scalar texture features can be introduced [2,4]:

1. Energy (second angular moment)

$$\boldsymbol{f_1} = \sum_{(\boldsymbol{i}, \boldsymbol{j}) \in \boldsymbol{I}^2} \boldsymbol{p}(\boldsymbol{i}, \boldsymbol{j})^2. \tag{7}$$

The function $\boldsymbol{x} \to \boldsymbol{x^2}$ is convex, hence more concentrated PDF $\boldsymbol{p}$ yields higher energy value. When the SGLDM entries concentrate around given intensities, it follows that the texture is uniform. Therefore, energy is a global measure of texture uniformity.

2. Contrast (inertia)

$$\boldsymbol{f_2} = \sum_{\boldsymbol{i} \in \boldsymbol{I}} \boldsymbol{i^2} \boldsymbol{p}_{\boldsymbol{x}-\boldsymbol{y}}(\boldsymbol{i}). \tag{8}$$

Contrast measures local texture non-uniformity because the weighting factor promotes far-from-diagonal regions of the SGLDM. Large values of such entries mean that locally there are many pixels pairs of significantly different grayscales. This happens, for example, when there are numerous sharp edges. Hence, off-diagonal SGLDMs yield higher values of $\boldsymbol{f_2}$ and contrast measures local texture non-uniformity.

3. Correlation

$$\boldsymbol{f_3} = \frac{\sum_{(\boldsymbol{i}, \boldsymbol{j}) \in \boldsymbol{I}^2} \boldsymbol{ijp}(\boldsymbol{i}, \boldsymbol{j}) - \boldsymbol{\mu_x \mu_y}}{\boldsymbol{\sigma_x \sigma_y}}, \tag{9}$$

where $\boldsymbol{\mu_x}$ and $\boldsymbol{\mu_y}$ are means $\boldsymbol{\sigma_x}$ and $\boldsymbol{\sigma_y}$ are standard deviations of the respective marginal distributions $\boldsymbol{p_x}$, $\boldsymbol{p_y}$. For SGLDM defined by (2) those distributions are equal, hence this feature is another measure of uniformity of $\boldsymbol{p}$.

4. Inverse difference moment (local uniformity)

$$\boldsymbol{f_5} = \sum_{(\boldsymbol{i}, \boldsymbol{j}) \in \boldsymbol{I}^2} \frac{\boldsymbol{1}}{\boldsymbol{1} + (\boldsymbol{i} - \boldsymbol{j})^2} \boldsymbol{p}(\boldsymbol{i}, \boldsymbol{j}) = \sum_{\boldsymbol{i} \in \boldsymbol{I}} \frac{\boldsymbol{1}}{\boldsymbol{1} + \boldsymbol{i^2}} \boldsymbol{p}_{\boldsymbol{x}-\boldsymbol{y}}(\boldsymbol{i}). \tag{10}$$

Opposed to contrast $\boldsymbol{f_2}$, we conclude that inverse difference moment measures local texture uniformity because the weighting factor promotes near-diagonal region of the SGLDM and damps influence of its far-from-diagonal regions. This happens when many pixels have neighbours of similar intensity. Hence, nearly-diagonal SGLDMs yield higher values of , and inverse $\boldsymbol{f_5}$ difference moment measures local texture uniformity.

5. Entropy

$$\boldsymbol{f_{11}} = -\sum_{\boldsymbol{i} \in \mathbf{supp}(\boldsymbol{p}_{\boldsymbol{x}-\boldsymbol{y}})} \boldsymbol{p}_{\boldsymbol{x}-\boldsymbol{y}}(\boldsymbol{i}) \,\mathbf{log}\, \boldsymbol{p}_{\boldsymbol{x}-\boldsymbol{y}}(\boldsymbol{i}). \tag{11}$$

The function $\boldsymbol{x} \to -\boldsymbol{x}\,\mathbf{log}\,\boldsymbol{x}$ is concave, hence more uniform, or constant, PDF $\boldsymbol{p}_{\boldsymbol{x}-\boldsymbol{y}}$ yields higher entropy value. This means that the more is the SGLDM spread along its diagonal, the higher value of $\boldsymbol{f_{11}}$. This happens when many pixels have neighbors of much different intensity. Therefore, the texture is disordered, and this definition mimics Gibbs entropy concept known in statistical mechanics.

In Haralick's work [5] fourteen texture features have been introduced, while above we have cited only five. Our choice of five features from the full set of fourteen is dictated by the fact that only five of them can be easily transferred to the colour domain while retaining their analogous perceptual motivation. The remaining nine features can also be transferred to the colour domain, however their meaning is yet unknown. Finding good perceptual motivation for those transferred features is left for future papers.

### 2.2. Colour Correlogram, Colour Cooccurrence Matrix, and Statistical Features for Colour Textures

Let $\boldsymbol{C}$ be the RGB colour cube and let $\boldsymbol{c}\colon \boldsymbol{C} \to \boldsymbol{I} = \{\boldsymbol{c_0}, \dots \boldsymbol{c_{N-1}}\}$ be any palette (has right inverse in the category of sets), and let $\boldsymbol{H}\colon \boldsymbol{X} \to \boldsymbol{I}$ be a colour texture. Using this notation we can define colour correlogram by the following formula:

$$\boldsymbol{CC^d(i,j) = Card\{(x,y) \mid x,y \in X, \rho(x,y) = d, H(x) = i, H(y) = j\}}, \tag{12}$$

We see that the above definition matches the one given by (2). However, the SGLDM and the colour correlogram differ substantially, and those differences stem from very different definition of $\boldsymbol{I}$. Although the palette range $\boldsymbol{I}$ is defined in an identical way as in Section 2 on the set level, it misses numerous additional structures which accompanied the set of graylevels. Namely, $\boldsymbol{I}$ has no natural ordering, hence every permutation of $\boldsymbol{I}$ induces a palette carrying equivalent information content, and there is no natural way to distinguish any such permutation. Also, $\boldsymbol{I}$ has no natural topology defining neighbouring colours. As a consequence, there is no metric on $\boldsymbol{I}$. Additionally, $\boldsymbol{I}$ has no natural linear structure allowing scaling, adding, and subtracting colours. In other words, there is no natural way to assess perceptual colour difference between $\boldsymbol{c_\alpha}$ and $\boldsymbol{c_{\alpha+1}}$, and actual relation of colours $\boldsymbol{c_\alpha}$ and $\boldsymbol{c_{\alpha+1}}$ is not perceptually connected with actual relation of colours $\boldsymbol{c_\beta}$ and $\boldsymbol{c_{\beta+1}}$ for any $\boldsymbol{\alpha \neq \beta}$.

In consequence, the above shortcomings of the palette range $\boldsymbol{I}$ do not allow to introduce not only features (7)–(11), but any features involving arithmetic operations on elements of $\boldsymbol{I}$. Although there is no possibility to define scalar features for any individual colour correlogram, metrics on a set of all colour correlograms (12) can be successfully defined. This metrics allow employing colour correlograms (12) for Content-Based Image Retrieval (CBIR) tasks [7, 10].

Now, let $\boldsymbol{C}$ be the HSV colour cone and let $\boldsymbol{I} \subset \boldsymbol{C}$ be an $\boldsymbol{\varepsilon}$-net in $\boldsymbol{C}$, which means that every element of $\boldsymbol{C}$ is not further than $\boldsymbol{\varepsilon}$ from some element of $\boldsymbol{I}$ (close-to-uniform quantization). Opposed to previous situation where $\boldsymbol{I}$ had no structure, here $\boldsymbol{I}$ inherits metric (and therefore also topology) and linear structure from the HSV colour space. Naturally, any colour texture consists now of three independent components, namely $\boldsymbol{H = (H_H, H_s, H_V)}$. Given this, we define multi-component colour cooccurrence matrix by the following formula [1,13]:

$$\boldsymbol{CCM^d_{AB}(i,j) = Card\{(x,y) \mid x,y \in X, \rho(x,y) = d, H_A(x) = i, H_B(y) = j\}}, \tag{13}$$

where $\boldsymbol{A,B} \in \{\boldsymbol{H,S,V}\}$. Basically, every colour cooccurrence matrix component $\boldsymbol{CCM^d_{AB}}$ is an SGLDM (2) and has properties identical to those of the SGLDM, and therefore we have six independent SGLDMs. Hence, for every such component texture features (7)–(11) can be computed. In total 30 features can be obtained in this way. However, mixed components ($\boldsymbol{A \neq B}$) cannot be given perceptual meaning. Still, those features can be successfully applied to classification of textures [1].

## 3. Definition and Theoretical Properties of the Perceptual Colour Correlogram and Its Statistical Features

When considering application of the above generalizations of the SGLDM to robot perception one immediately encounters conceptual problems because either there are no understandable features, like in the case of colour correlogram, or such features have no clear perceptual interpretation comparable to (7)–(11) for grayscale textures. This motivates us to define perceptual colour correlogram and its respective statistical features which are free of this flaw.

The first step to accomplish this task is to choose proper colour space in which all colour components are easily interpretable in perceptual terms. It is most convenient to use the CIELab colour space $\boldsymbol{C}$ [8] which is tailored for this task. The next step is to choose a proper finite subset $\boldsymbol{I}$ of $\boldsymbol{C}$ which will serve as actual colour range for textures. A good starting point is to observe that all desired mathematical properties of $\boldsymbol{I}$ are assured when we choose $\boldsymbol{I}$ to be an $\boldsymbol{\varepsilon}$-net in $\boldsymbol{C}$. In order to quantize the colour space $\boldsymbol{C}$ uniformly in perceptual terms we assume that $\boldsymbol{C}$ has metric structure induced by any perceptual colour difference function $\Delta\boldsymbol{E}$ from the range of $\Delta\boldsymbol{E}$'s described in [8]. Additionally, we assume that the coordinate-wise projection of the set $\boldsymbol{I}$ onto its $\boldsymbol{L^*}$ component forms a set $\boldsymbol{I_{L^*}}$ which is metrically uniform. This property assures that the analogy between $\boldsymbol{I_{L^*}}$ and the set of graylevels is complete.

Let $\boldsymbol{H}\colon \boldsymbol{X} \to \boldsymbol{I}$ be a colour texture and let $\Delta\boldsymbol{E}\colon \boldsymbol{C} \to \mathbb{R}_{\geq 0}$ be any perceptual colour difference function. We define the perceptual colour correlogram $\boldsymbol{PPC^d}$ by means of the following formula:

$$\boldsymbol{PPC^d(i,\alpha) = Card\{(x,y) \mid x,y \in X, \rho(x,y) = d, H(x) = i, \Delta E(H(x), H(y)) = \alpha\}}, \tag{14}$$

where $\boldsymbol{d}$ is a free parameter. It is straightforward that $\boldsymbol{PPC^0}$ is zero except for the line $\boldsymbol{\alpha = 0}$ and this line is simply the histogram of the texture component $\boldsymbol{H_{L^*}}$. Therefore the perceptual colour correlogram should be considered as a generalization of $\boldsymbol{L^*}$ component of colour texture histogram. It the subsequent text we will omit the superscript $\boldsymbol{d}$ as far as it is clear which particular value of $\boldsymbol{d}$ is being concerned or when value of $\boldsymbol{d}$ is arbitrary.

The perceptual colour correlogram is also connected to the SGLDM by a simple relation. Namely, when the texture $\boldsymbol{H}$ is actually gray, which means that $\boldsymbol{H_{a^*} = H_{b^*} = 0}$, the perceptual colour correlogram (14) of and the SGLDM (2) of the $\boldsymbol{H_{L^*}}$ are related by the following formula:

$$PPC^d(i,\alpha) = M(i, i+\alpha) + M(i, i-\alpha), \quad (15)$$

because we assumed previously that the $I_{L^*}$ set is metrically uniform and $\Delta E$ is a non-negative metric. It is easily seen that the perceptual colour correlogram has all the desired properties and none of the drawbacks pointed out in Section 2.2: it's both dimensions have natural order, topology, linear structure, and metric structure consistent with human perception of colours.

In order to proceed any further we have to define the following PDFs induced by the PPC:

$$pp(i,\alpha) = \frac{PPC(i,\alpha)}{\sum_{k,\beta} PPC(k,\beta)}, \quad (16)$$

$$pp_x(\alpha) = \sum_{i \in I} pp(i,\alpha) = p_{x-y}(\alpha). \quad (17)$$

The second equality in the above equation states that the marginal distribution $pp_x$ equals the marginal distribution $p_{x-y}$ for the SGLDM.

Now, we are ready to define statistical features of the perceptual colour correlogram:

1. Energy (second angular moment)

$$\widetilde{f_1} = \sum_{i,\alpha} pp(i,\alpha)^2. \quad (18)$$

Concentrated PDF $pp$ yields higher energy value. When PPC entries concentrate around fixed $L^*$ and $\Delta E$ values, it can be shown that the texture is uniform. Therefore, energy is a global measure of colour texture uniformity.

2. Contrast (inertia)

$$\tilde{f}_2 = \sum_i i^2 pp_x(i). \quad (19)$$

Contrast measures local texture non-uniformity because the weighting factor promotes the region of the PPC for which $\Delta E$ is large. Large values of such entries mean that locally there are many pixels pairs of significantly different colours.

3. Correlation

$$\widetilde{f_3} = \frac{\sum_{i,\alpha} i\alpha pp(i,\alpha) - \mu_x\mu_y}{\sigma_x\sigma_y}, \quad (20)$$

where $\mu_x$ and $\mu_y$ are means $\sigma_x$ and $\sigma_y$ are standard deviations of the respective marginal distributions $pp_x$, $pp_\alpha$, where the latter marginal distribution is defined in the same manner as $pp_x$. By its definition, correlation measures constancy of $pp$.

4. Inverse difference moment (local uniformity)

$$\widetilde{f_5} = \sum_i \frac{1}{1+i^2} pp_x(i). \quad (21)$$

Opposed to contrast $\widetilde{f_2}$, we conclude that inverse difference moment measures local colour texture uniformity.

5. Entropy

$$\widetilde{f_{11}} = -\sum_{i \in \mathrm{supp}(pp_x)} pp_x(i) \log pp_x(i). \quad (22)$$

The more is the PPC is spread along its $\Delta E$-dependent dimension, the higher value of $\widetilde{f_{11}}$. This happens when many pixels have neighbors of many different colours. Such colour textures are highly disordered.

Hereby we have defined five statistical features of the perceptual colour correlogram and we have proved that these features have perceptual interpretation.

## 4. Results of Numerical Experiments on Natural Colour textures

The features (18)–(22) introduced above clearly generalize Haralick's features (7)–(11). Hence, it is expected that they should have strong discriminative power for colour textures. In order to check whether this statement is actually true, we have used MIT's vismod texture database [14]. Two examples of these textures are shown in the figure below.

*Fig. 1. The top image shows colour texture of beans, while the bottom image shows colour texture of coffee*

Both images have been acquired in the similar lightning conditions and using the same exposure parameters. Resolution of both images is $512 \times 512$. Acquired texture resolution implies that each texture consists of 262,144 pixels and contains numerous characteristic microstructure cells. Therefore, description of such a texture in statistical terms is reasonable.

For textures shown in Fig. 1 the SGLDMs were calculated, and conversion to grayscale has been achieved by dropping $\boldsymbol{a}^*$ and $\boldsymbol{b}^*$ components of textures after transforming it to the CIELab colour space. Exemplary SGLDM surface plot and PPC surface plot is shown in the figure below.

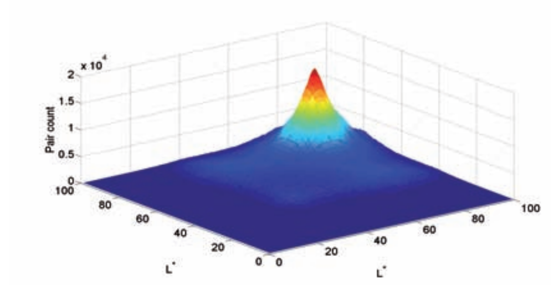


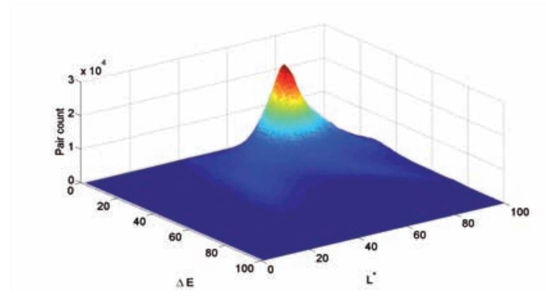


***Fig. 2. The top plot contains the SGLDM of the $L^*$ component of the upper texture depicted in Fig. 1. The lower plot contains the PPC of the upper texture depicted in Fig. 1***

During calculation of the above PPC, simplest possible definition of colour difference measure was used. Hence, the colour difference was simply Euclidean distance in the CIELab colour space. For both SGLDM and PPC the free distance parameter $\boldsymbol{d}$ was set to 30 pixels. This value is larger than typical microstructure cell size (here – grain size), hence summation related to cardinality operator in the definition of the SGLDM and the PPC was running over several microstructure cells.

In the above figure it is clearly visible that the PPC is skew along its $\Delta\boldsymbol{E}$ dimension while there is no significant skewness in the SGLDM, and the SGLDM is almost rotationally symmetric. Such phenomenon was observed for all investigated textures of approximately symmetric histogram of intensity, and the reason for this is explained by the relation (15) of both matrices.

The PPC attains a broad maximum at $\Delta\boldsymbol{E} \approx \mathbf{9}$ which means that the investigated texture is perceptually non-uniform. This follows directly from the very definition of $\Delta\boldsymbol{E}$: when $\Delta\boldsymbol{E} > 5$ it means that a not trained observer easily sees significant colour difference.

For both texture classes shown in Fig. 1, Haralick's features (7)–(11) and proposed features (18)-(22) were calculated. Values of these features are assembled in the table below.

| Feature | Coffee texture in Fig. 1 | Beans texture in Fig. 1 |
|---|---|---|
| $f_1$ | $4.2\times10^{-4}$ | $5.2\times10^{-4}$ |
| $\tilde{f}_1$ | $6.0\times10^{-4}$ | $8.2\times10^{-4}$ |
| $f_2$ | $5.0\times10^{2}$ | $5.1\times10^{2}$ |
| $\tilde{f}_2$ | $7.5\times10^{2}$ | $6.7\times10^{2}$ |
| $f_3$ | $8.8\times10^{-6}$ | $8.6\times10^{-6}$ |
| $\tilde{f}_3$ | $-4.3\times10^{-6}$ | $9.1\times10^{-6}$ |
| $f_5$ | $6.2\times10^{-2}$ | $6.9\times10^{-2}$ |
| $\tilde{f}_5$ | $1.0\times10^{-1}$ | $1.5\times10^{-1}$ |
| $f_{11}$ | 3.8 | 3.8 |
| $\tilde{f}_{11}$ | 4.0 | 3.9 |

***Tab. 1. List of mean values of Haralick features and proposed features for textures shown in Fig. 1***

Values shown in the above table prove that the proposed features can discriminate textures shown in Fig. 1. It must be noted that differences among colour features (18)–(22) for both texture classes are larger than differences among respective grayscale features (7)–(11). This can be explained by the fact that the investigated texture classes are more distinct when colour components are retained than when those components are disregarded; it has been observed that the beans texture is more uniform mainly in its component, while its colour components are very similar to these of coffee texture.

Hereby we have shown an example of natural colour textures for which the proposed features (18)–(22) express discriminatory capabilities not worse Haralick features (7)–(11). More extensive test for larger set of colour texture classes will be performed in future. Also, in coming research it will be investigated whether the proposed features (18)–(22) allow to discern textures which cannot be separated by Haralick's features (7)–(11).

## 5. Summary

In this paper we introduced a novel type of colour correlogram, the perceptual colour correlogram, generalizing concept of the spatial graylevel dependency matrix (SGLDM) to the case of colour textures. For construction of the perceptual colour correlogram we used the $\Delta\boldsymbol{E}$ measure describing perceptual colour difference. Therefore it became possible to interpret the introduced colour correlogram in perceptual terms. The PDF induced by the perceptual colour correlogram was used to define five statistical features generalizing Haralick features of the SGLDM. These features can be used for colour texture classification or statistical modelling.

It is planned to investigate the introduced statistical features more thoroughly in order to gain deeper understanding of their relations to Haralick features. This understanding should prove useful to define further perceptual colour correlogram features. Also, extensive numerical experiments should be conducted to test actual discriminative power of the introduced statistical features. Moreover, it seems that the proposed features can be easily generalized to account for texture orientation parameter $\boldsymbol{\theta}$ (horizontal, vertical, and two diagonals) present in the generalized SGLDM.

In future works the proposed features will be compared to state-of-the-art features, like Gabor-filter features present in MPEG-7 texture descriptor.

## ACKNOWLEDGEMENTS

This work was supported by "Autonomy in rescue and exploration robots", RobREx, realized for The National Centre for Research and Development, grant number PBS1/A3/8/2012.

## AUTHOR

**Konrad Bojar –** Laboratory of Autonomous Defense Systems, Industrial Research Institute for Automation and Measurements PIAP, Al. Jerozolimskie 202, 02-486 Warsaw, Poland.
E-mail: kbojar@piap.pl, www: http://www.piap.pl.

## REFERENCES

[1] Arvis V. et al., "Generalization of the cooccurrence matrix for colour images: application to colour texture classification", *Image Analysis & Stereology*, vol. 23, 2004, 63–72. DOI: 10.5566/ias.v23.p63-72.

[2] Berry J., Goutsias J., "A comparative study of matrix measures for maximum likelihood texture classification", *IEEE Transaction on Systems, Man and Cybernetics*, vol. 21, no. 1, 1991, 252–261. DOI: 10.1109/21.101156.

[3] Bojar K., Nieniewski M., "Analysis of temporal variations of dynamic textures by means of the SGLDM with application to solar EIT images", Machine Graphics & Vision, 2008, vol. 17, no. 3, 219–247.

[4] Dixit A., Hedge N. P., "Image Texture Analysis Techniques – Survey", *3rd International Conference on Advanced Computing & Communication Technologies*, Rohtak, April 6–7, 2013. DOI 10.1109/ACCT.2013.49.

[5] Haralick R., Shanmugam K., Dinstein I., "Textural features for image classification", *IEEE Transactions on Systems, Man and Cybernetics*, vol. 3, no. 6, 1973, 610–621. DOI: 10.1109/TSMC.1973.4309314.

[6] Huang J. et al., "Spatial Colour Indexing and Applications", *International Journal of Computer Vision*, vol. 35, no. 3, 1999, 245–268. DOI: 10.1023/A:1008108327226.

[7] Kiranyaz S., Birinci M., Gabbouj M., "Perceptual colour descriptor based on spatial distribution: A top-down approach", *Image and Vision Computing*, vol. 28, 2010, 1309–1326. DOI: 10.1016/j.imavis.2010.01.012.

[8] Melgosa M., "Testing CIELAB-based colour difference formulas", *Colour Research and Application*, vol. 25, 2000, no. 1, 49–55. DOI: 10.1002/(SICI)1520-6378(200002)25:1<49::AID-COL7>3.0.CO;2-4.

[9] Nanni L., Lumini A., Branham S., "Survey on LBP based texture descriptors for image classification", Expert Systems with Applications, Vol. 39, 2013, 3634–3641. DOI: 10.1016/j.eswa.2011.09.054.

[10] S. Shim, T. Choi, "Image indexing by modified colour cooccurrence matrix". In: *Acoustics, Speech,* and *Signal Processing. Proceedings*, Hong Kong, April 6–10, 2003, vol. 3, III–577. DOI: 10.1109/ICASSP.2003.1199540.

[11] Swain M., Ballard D., "Colour indexing", *International Journal of Computer Vision*, vol. 7, no. 1, 1991, 11–32. DOI: 10.1007/BF00130487.

[12] Raheja J., Ajay B., Chaudhary, "Real time fabric defect detection system on an A. embedded DSP platform", *Optik-International Journal for Light and Electron Optics*, 2013, vol. 124, no. 21, 5280–5284. DOI: 10.1016/j.ijleo.2013.03.038.

[13] Vadivel A., Sural S., Majumdar A., "An integrated colour and intensity cooccurrence matrix", *Pattern Recognition Letters*, 2007, vol. 28, 974–983. DOI: 10.1016/j.patrec.2007.01.004.

[14] http://vismod.media.mit.edu/pub/VisTex/VisTex.tar.gz, MIT Texture Database, accessed on 13 Dec. 2014.